https://ijac.journals.pnu.ac.ir/

Iranian Journal of Analytical Chemistry

Volume 13, Issue 1, Spring 2026, Pages 93-108

DOI: 10.30473/ijac.2026.78706.1354

OPEN ACCESS

Iranian Journal of Analytical Chemistry

Research Article

Evaluation of the Efficiency of Magnetic Iron Oxide Nanoparticles for the Removal of Heavy Metals from Industrial Wastewater

Hamid Yazdani ✉

Assocate Professor Department of Chemical Engineering, Payame Noor Uiversity, Tehran, Iran.

✉ **Correspondence:**
Hamid Yazdani
Email: h.yazdani@pnu.ac.ir

Received: 21 Aug 2026
Accepted: 11 Oct 2026

A B S T R A C T

Heavy metals such as lead, nickel, and cadmium present in industrial wastewater pose serious environmental and public health risks. In this study, magnetic iron oxide nanoparticles with a crystallite size of 18 nm were synthesized via a co-precipitation method and evaluated for the simultaneous removal of Pb(II), Ni(II), and Cd(II) from aqueous solutions. Characterization was performed using X-ray diffraction (XRD), optical microscopy, and magnetization measurements. Batch adsorption experiments were conducted at 25 °C to investigate the effects of pH (3–9), adsorbent dosage (0.3–1.0 g/L), and contact time (5–30 min). The key novelty of this work is the achievement of high removal efficiencies under acidic conditions (pH = 3) without any surface modification: 97% for Pb(II), 98% for Ni(II), and 91% for Cd(II), indicating strong potential for treating acidic industrial effluents without pH adjustment. Increasing the pH to 9 reduced the removal efficiencies to 45% for Pb(II), 58% for Ni(II), and 41% for Cd(II).The optimal adsorbent dosage was determined to be 0.5 g/L; higher dosages reduced efficiency due to particle agglomeration. Adsorption equilibrium was reached within 25–30 minutes. Kinetic data showed an excellent fit with the pseudo-second-order model, while equilibrium data were well described by the Langmuir isotherm, indicating monolayer chemisorption on homogeneous adsorption sites. The maximum adsorption capacities were 3.42, 7.28, and 1.41 mg/g for Pb(II), Ni(II), and Cd(II), respectively. Rapid magnetic separation and reusability make these nanoparticles an efficient and cost-effective adsorbent for the treatment of industrial wastewater.

K E Y W O R D S

Iron oxide nanoparticles, heavy metal removal, wastewater treatment, adsorption, magnetic separation, industrial effluent.

How to cite

H. Yazdani, Evaluation of the Efficiency of Magnetic Iron Oxide Nanoparticles for the Removal of Heavy Metals from Industrial Wastewater, *Iran. J. Anal. Chem.* 13 (2026) 93-108. (DOI:10.30473/ijac.2026.78706.1354)

Copyright © 2026 The Authors. Published by Payame Noor University.

This work is licensed under a Creative Commons Attribution-NonCommercial 4.0 International license (https://creativecommons.org/licenses/by-nc/4.0/). Non-commercial uses of the work are permitted, provided the original work is properly cited.

Introduction

Contamination of surface and groundwater by heavy metals has become a major environmental challenge. Heavy metals such as lead, cadmium, mercury, chromium, nickel, and copper can pose serious risks to human health and aquatic ecosystems because of their toxicity, persistence, and potential for bioaccumulation [1-3]. Various industries, including metal plating, dyeing, leather processing, battery manufacturing, mining, and petrochemical activities, are important sources of wastewater containing heavy metals [4,5]. The discharge of these pollutants into water resources, even at relatively low concentrations, can cause adverse toxicological effects [1-3]. Conventional methods for treating industrial wastewater include chemical precipitation, ion exchange, membrane processes, electrochemical methods, and adsorption [6,7]. However, these technologies can have limitations such as chemical consumption, sludge generation, operating cost, and reduced efficiency under some wastewater conditions [6,7]. Among these methods, adsorption has attracted considerable attention because of its operational simplicity, relatively low cost, and effectiveness for removing dissolved contaminants [8,9]. Nanomaterials have also emerged as important adsorbents in water and wastewater treatment because of their high surface area, surface reactivity, and tunable surface properties [8-11]. Magnetic iron oxide nanoparticles, particularly magnetite (Fe_3O_4), have received considerable attention because their magnetic properties facilitate separation from aqueous media, while their surface chemistry can support interactions with dissolved contaminants [9,12,13]. These characteristics can facilitate adsorbent recovery and reuse [12,13]. Heavy-metal removal by iron-oxide-based materials can involve adsorption, surface complexation, ion exchange, and other surface-mediated interactions, depending on the material and solution chemistry [9,13]. Surface hydroxyl groups (–OH) are important reactive sites in these interactions [9]. Surface modification with polymers, graphene-based materials, ionic liquids, or other functional materials can further alter adsorption capacity, selectivity, and stability [14-17]. Numerous studies have investigated nanostructured materials for heavy-metal removal. Zhang et al. reported arsenite and arsenate adsorption on $MnFe_2O_4$ and $CoFe_2O_4$ magnetic nanomaterials [18]. Kumar and Jiang investigated chitosan-functionalized graphene oxide for arsenic adsorption from aqueous solution [14]. Li et al. reported a magnetic cyclodextrin–chitosan/graphene-oxide-based adsorbent for chromium removal [15]. Several operational parameters influence adsorption performance, including solution pH, adsorbent dosage, contact time, initial pollutant concentration, temperature, and competing species [19-21]. Optimization of these parameters is important for maximizing removal efficiency while limiting adsorbent consumption and process costs [19,20]. Adsorption isotherm models such as Langmuir and Freundlich, together with kinetic models such as pseudo-first-order and pseudo-second-order models, are widely used to characterize adsorption behavior and estimate adsorption parameters [19,21]. In addition to adsorption performance, adsorbent stability and reusability are important for practical applications. Previous studies have investigated magnetic and other nanostructured adsorbents for repeated adsorption and desorption and for recovery of adsorbed metals [22,23]. Desorption can be performed using acidic or alkaline media, depending on the adsorbent and target metal [19,24]. Important challenges in nanomaterial-based wastewater

treatment include nanoparticle aggregation, loss of effective surface area, stability under operating conditions, and scale-up and cost considerations [8,13]. Recent research has therefore increasingly explored green synthesis routes, surface modification with biocompatible materials, and multifunctional nanocomposites [17,26,27]. Considering the growing importance of industrial wastewater treatment, the aim of this study is to evaluate the performance of magnetic iron oxide nanoparticles for the removal of heavy metals from industrial wastewater. This research investigates the effects of operational parameters, explores adsorption behavior, models adsorption isotherms and kinetics, and evaluates the practical applicability of the adsorbent. The present study evaluates Pb(II), Ni(II), and Cd(II) as the target metal ions. The removal capability of the unmodified Fe_3O_4 nanoparticles toward other metal ions was not investigated in the present work and should therefore be evaluated in future studies to establish broader applicability.

Recent studies further demonstrate the diversity of pollutant-removal approaches. Ionic-liquid-modified nano-clays have been investigated for Cd(II) removal, while modified nano-clay systems have also been evaluated for Pb(II) and Hg(II) removal [16,28]. Nickel removal has been studied using zinc-powder cementation under optimized operating conditions [29], and a magnetized tomato-residue-derived nanoadsorbent has recently been reported for Ni(II) removal from dairy wastewater [32]. In addition, an Ag-assisted ionic-liquid extraction system has been developed for the removal of an organic dye from environmental and pharmaceutical samples [31]. These studies broaden the context for comparing adsorption and separation strategies for both inorganic and organic pollutants.

Materials and Methods

1. Materials and Chemicals

Magnetic iron oxide nanoparticles (Fe_3O_4) with a purity of 99% and an average particle size of 18 nm were purchased from Merck, Germany [13,25]. The nanoparticles exhibited spherical morphology, a density of 5.31 g/cm³, and a black appearance. Sodium hydroxide (NaOH) and sulfuric acid (H_2SO_4) solutions (0.1 M) were used to adjust the pH of the solutions [9]. All chemicals used in this study were of analytical grade and were used without further purification.

2. Characterization of Nanoparticles

The crystalline structure and purity of the iron oxide nanoparticles were confirmed using X-ray diffraction (XRD) analysis [8]. The XRD pattern indicated that the nanoparticles possessed a high-purity inverse spinel structure characteristic of magnetite (Fe_3O_4). The average crystallite size was calculated using the Scherrer equation (Eq. 2) and was determined to be approximately 18 nm. The morphology and particle size distribution were examined using a Nikon E200 optical microscope [13].

3. Preparation of Industrial Wastewater Samples

Real wastewater samples were collected from a refinery located in southern Iran. The wastewater contained various concentrations of heavy metals along with other pollutants; however, the focus of the present study was on heavy metal contaminants. Table 1 presents the complete composition of the investigated wastewater [12,13,32]. After collection, the samples were stored at room temperature (approximately 25 °C), and their initial pH was measured prior to the adsorption experiments.

Table 1. Characteristics of Industrial Wastewater

Pollutants	(Pb^{2+})	(Ni^{2+})	(Cd^{2+})	(NO_3^-)	(PO_4^{3-})	Asphaltine	Turbidity
Initial Concentration	17	36	8	34	14	5	40
Unit	mg/L	mg/L	mg/L	mg/L	mg/L	Wt%	NTU

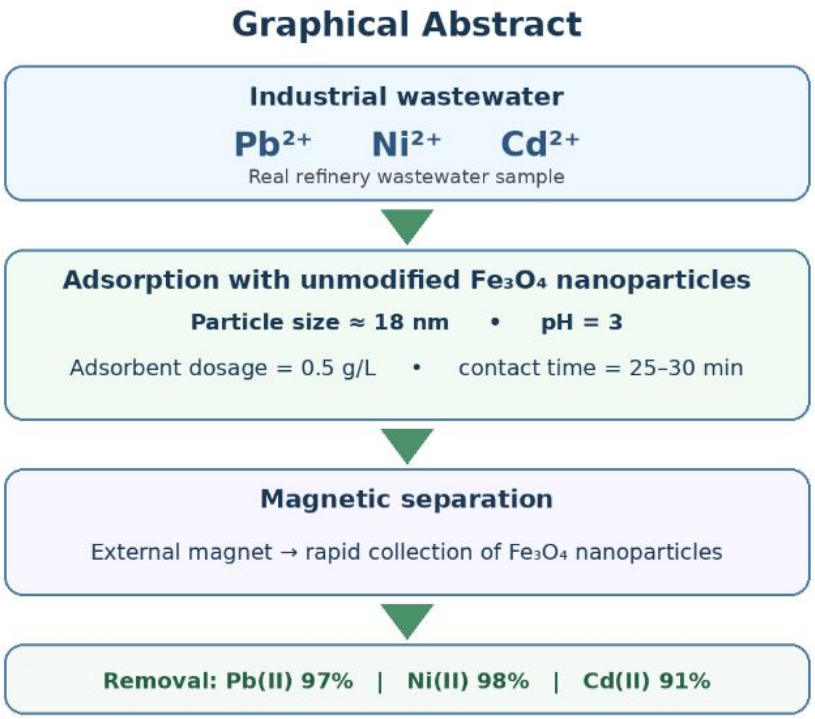

Figure 1. Graphical abstract of the adsorption process and key experimental steps for the removal of Pb(II), Ni(II), and Cd(II) using unmodified magnetic Fe_3O_4 nanoparticles.

4. Adsorption Experiments

Batch adsorption experiments were carried out to evaluate the removal performance of the magnetic iron oxide nanoparticles [9,13]. In each experiment, a fixed volume of wastewater (200 mL) was mixed with a specified amount of iron oxide nanoparticles (0.5 g). The suspensions were stirred using a magnetic stirrer for different contact times ranging from 5 to 30 minutes at room temperature [13].After equilibrium was reached, the nanoparticles were separated from the solution using an external magnet [19,21]. The residual concentrations of heavy metals in the supernatant were then measured using appropriate analytical methods.

4.1. Effect of pH

To investigate the effect of pH on the removal efficiency of heavy metals, adsorption experiments were conducted at four different pH values (3, 5, 7, and 9) [9,15]. The solution pH was measured using a Corning 430 pH meter and adjusted by adding 0.1 M NaOH or H_2SO_4 solutions. In these experiments, the adsorbent dosage was fixed at 0.5 g/L and the contact time was maintained at 30 minutes.

4.2. Effect of Adsorbent Dosage

The influence of nanoparticle dosage on heavy metal removal efficiency was investigated using different adsorbent dosages of 0.3, 0.5, 0.8, and 1.0 g/L ([8,20]). During these experiments, the

solution pH was maintained at the optimum value (pH = 3), and the contact time was fixed at 30 minutes.

4.3. Effect of Contact Time

To determine the adsorption equilibrium time, experiments were conducted over a contact time range of 5 to 30 minutes [20,23]. In this stage, both the pH and adsorbent dosage were maintained at their optimum values. Samples were collected at contact times of 5, 10, 15, 20, 25, and 30 minutes.

5. Analytical Methods

The concentrations of heavy metals (lead, nickel, and cadmium) were measured using a Hach DR2800 spectrophotometer.

6. Calculation of Removal Efficiency

The removal efficiency ® of heavy metals was calculated using the following equation ([9,13]) (Eq. 1):

$$R(\%) = \frac{C_0 - C_e}{C_0} \times 100 \quad (1)$$

where:

C_0 = initial concentration of the heavy metal (mg/L)

C_e = equilibrium concentration of the heavy metal after adsorption (mg/L)

7. Data Analysis

All experiments were conducted in five replicates, and the results are reported as mean ± standard deviation. Statistical analysis was performed using Microsoft Excel software. To investigate the adsorption mechanism, the experimental data were fitted to adsorption isotherm models (Langmuir and Freundlich) as well as kinetic models (pseudo-first-order and pseudo-second-order) [2.20.34].

Results and Discussion

1. Characterization of Iron Oxide Nanoparticles

The magnetic iron oxide nanoparticles (Fe_3O_4) were characterized using several analytical techniques prior to the adsorption experiments. The X-ray diffraction (XRD) pattern of the synthesized nanoparticles is presented in Figure 2. Characteristic diffraction peaks were observed at 2θ values of 30.1°, 35.5°, 43.1°, 53.4°, 57°, and 62.6°, corresponding to the crystal planes (220), (311), (400), (422), (511), and (440), respectively, of the cubic spinel structure of magnetite (Fe_3O_4) [11,27].The absence of impurity peaks confirmed the high purity (>99%) of the synthesized nanoparticles. Using the Scherrer equation, the average crystallite size was estimated to be approximately 18 nm, which was consistent with the specifications provided by the manufacturer (Merck, Germany) [13].

$$D = \frac{K\lambda}{\beta cos\theta} \quad (2)$$

where D is the crystallite size, K is the Scherrer constant (0.9), λ is the X-ray wavelength (1.5406 Å), β is the full width at half maximum (FWHM) of the diffraction peak, and θ is the Bragg angle. Optical microscopy images obtained using a Nikon E200 microscope revealed that the nanoparticles possessed an approximately spherical morphology with a relatively uniform size distribution. The strong magnetic properties of the nanoparticles enabled their rapid and complete separation from the wastewater solution using an external magnet, which represents one of the major advantages of this adsorbent for industrial applications [9,13].

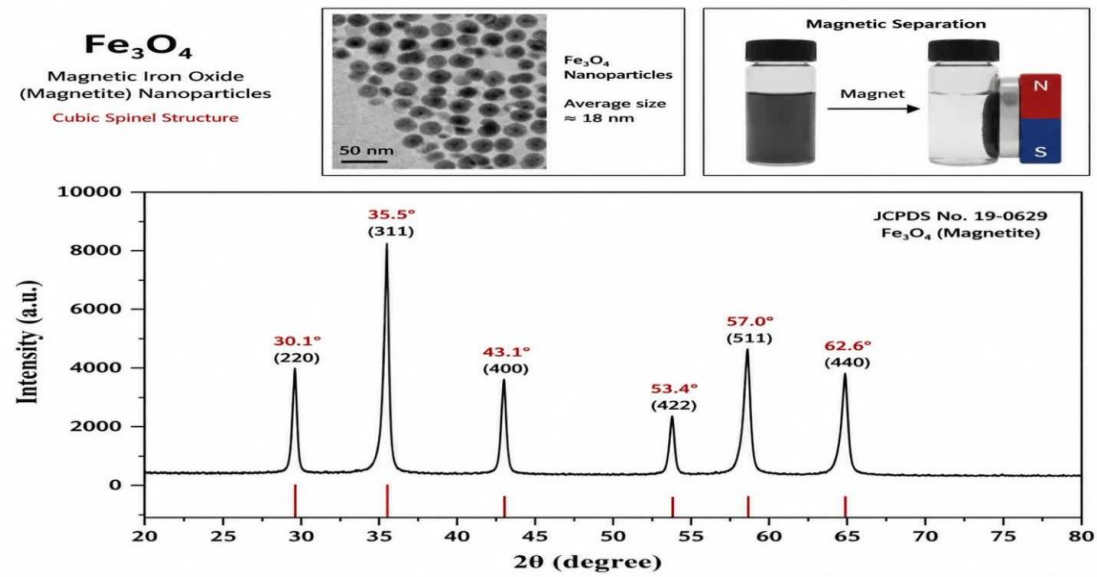

Figure 2. XRD pattern of synthesized Fe_3O_4 magnetic nanoparticles showing characteristic peaks corresponding to the cubic spinel structure of magnetite.

2. Effect of pH on the Removal Efficiency of Heavy Metals

Solution pH is one of the most important parameters affecting the adsorption process of heavy metals, as it influences the surface charge of the adsorbent, the degree of ionization of surface functional groups, and the chemical speciation of metals in solution [7,12]. The effect of pH on the removal efficiency of lead, nickel, and cadmium was investigated within the pH range of 3–9 (adsorbent dosage: 0.5 g/L, contact time: 30 min, room temperature). The results are presented in Figure 2 and Table 2.

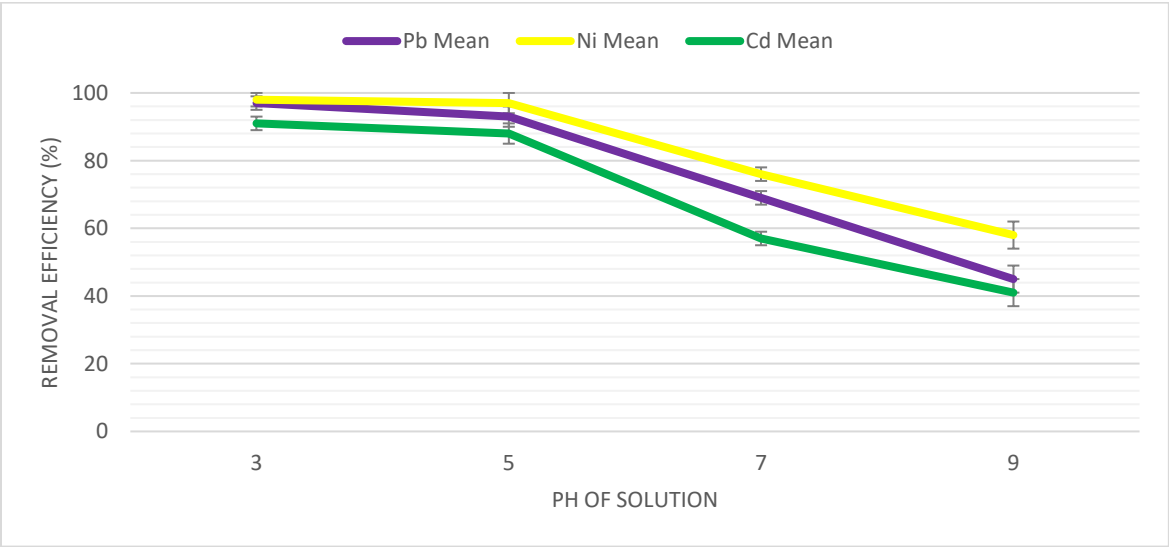

Figure 3. Effect of pH on the removal efficiency of Pb(II), Ni(II), and Cd(II) by Fe_3O_4 magnetic nanoparticles (adsorbent dose: 0.5 g/L, contact time: 30 min, initial concentrations: Pb=17 mg/L, Ni=36 mg/L, Cd=8 mg/L, temperature: 25±2°C, n=5).

Table 2. Effect of pH on removal efficiency of heavy metals by Fe_3O_4 nanoparticles.

pH	3	5	7	9
Pb(II) Removal(%)	97	93	69	45
Ni(II) Removal(%)	98	97	76	58
Cd(II) Removal(%)	91	88	57	41

As shown in Figure 3, the highest removal efficiency for all three metals was achieved at pH = 3. At this pH, the removal efficiencies of lead, nickel, and cadmium were 97%, 98%, and 91%, respectively. Increasing the pH from 3 to 5 resulted in a slight decrease in removal efficiency (lead: 93%, nickel: 97%, cadmium: 88%). Further increases in pH to 7 and 9 caused a significant reduction in removal efficiency; at pH = 9, the removal efficiencies of lead, nickel, and cadmium decreased to 45%, 58%, and 41%, respectively. This inverse trend (decreasing removal efficiency with increasing pH) can be explained by the following mechanisms:

1. Formation of Anionic Metal Complexes at Low pH

In acidic environments (pH < 4), heavy metals may exist as anionic or neutral complexes such as $PbCl^+$, $Pb(OH)^+$, $NiCl^+$, and $CdCl^+$ [13,15]. These species can be adsorbed through electrostatic attraction or surface complex formation with the hydroxyl groups present on the nanoparticle surface (≡Fe–OH) [8].

2. Positive Surface Charge of Nanoparticles at Low pH

At pH values below the point of zero charge, the nanoparticle surface becomes positively charged due to protonation of surface hydroxyl groups. However, in the presence of chloride or sulfate anions (present in the wastewater), heavy metals may form anionic or neutral complexes and become adsorbed through specific adsorption or inner-sphere surface complexation mechanisms [21,22]. This mechanism is independent of surface charge and becomes dominant under acidic conditions.

3. Competition of Hydrogen Ions and Hydroxide Precipitation at High pH

With increasing pH, two major factors contribute to the reduction in adsorption efficiency:

❖ Hydrogen ion competition:

At higher pH values, the concentration of H^+ ions decrease, and the nanoparticle surface becomes deprotonated, acquiring a negative charge. Although this negative charge would theoretically enhance the adsorption of metal cations, in practice, precipitation of metal hydroxides at high pH causes metals to be removed from solution through precipitation rather than surface adsorption [12,13]. These precipitates may block active surface sites and reduce the actual adsorption efficiency.

❖ Changes in metal speciation:

At high pH values, metals tend to form soluble hydroxide species with lower affinity for surface adsorption [21].

4. Comparison Among Metals

Nickel exhibited higher removal efficiency than lead and cadmium throughout the investigated pH range. This behavior can be attributed to the smaller ionic radius of nickel (0.69 Å) compared with lead (1.19 Å) and cadmium (0.95 Å), as well as its greater tendency to form stable complexes [21,22]. Based on the obtained results, pH = 3 was selected as the optimum pH

for heavy metal removal, since the highest removal efficiencies (>90% for all three metals) were achieved under this condition.

3. Effect of Adsorbent Dosage on Removal Efficiency

The effect of adsorbent dosage on the removal efficiency of heavy metals was investigated within the range of 0.3–1.0 g/L (pH = 3, contact time: 30 min, room temperature). The results are presented in Figure 4.

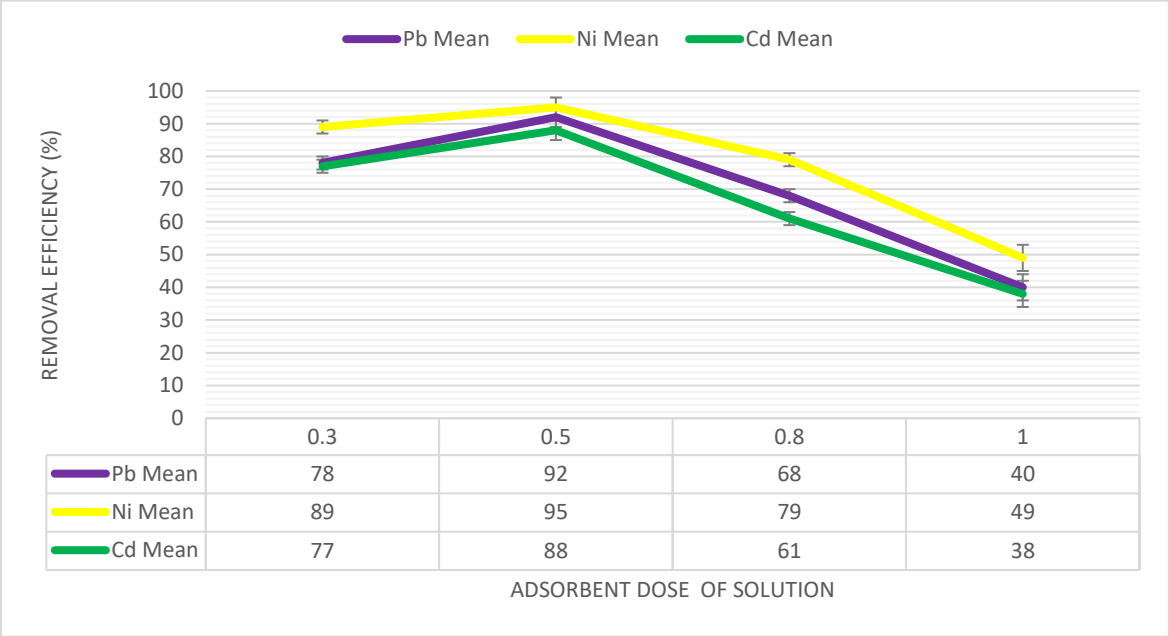

Figure 4. Effect of adsorbent dose on the removal efficiency of Pb (II), Ni (II), and Cd (II) by Fe_3O_4 magnetic nanoparticles (pH=3, contact time: 30 min, initial concentrations: Pb=17 mg/L, Ni=36 mg/L, Cd=8 mg/L, temperature: 25±2°C, n=5).

With increasing adsorbent dosage from 0.3 to 0.5 g/L, the removal efficiency of lead increased from 78% to 92%, nickel from 89% to 95%, and cadmium from 77% to 88%. This significant improvement can be attributed to the increase in the number of active adsorption sites and the greater specific surface area available for adsorption of metal ions [9,18]. How ever, further increasing the adsorbent dosage to 0.8 and 1.0 g/L resulted in a considerable decline in removal efficiency. At a dosage of 1.0 g/L, the removal efficiencies of lead, nickel, and cadmium decreased to 40%, 49%, and 38%, respectively. This unexpected reduction can be explained by the following mechanisms:

1. Saturation of Adsorption Sites and Decrease in Metal-to-Adsorbent Ratio

At high adsorbent dosages, the ratio of metal concentration to adsorbent surface area decreases. In other words, the number of available metal ions becomes insufficient to occupy all adsorption sites, leaving a significant portion of the sites unoccupied [8,19]. This phenomenon reduces the adsorbent utilization efficiency.

2. Aggregation and Agglomeration of Nanoparticles

At high adsorbent concentrations, nanoparticles tend to aggregate and form agglomerates, leading to a reduction in effective specific surface area and blockage of internal adsorption sites [8,13]. In addition, agglomeration may

limit the mass transfer of metal ions to the nanoparticle surface.

3. Increase in Turbidity and Interference with Measurements

At high adsorbent dosages, solution turbidity increases, which may affect the accuracy of residual metal concentration measurements using the spectrophotometer [20]. From both economic and adsorbent optimization perspectives, a dosage of 0.5 g/L was selected as the optimum dosage, since this condition provided the highest removal efficiencies (lead: 92%, nickel: 95%, cadmium: 88%) with minimum adsorbent consumption [13,22].

4. Effect of Contact Time and Adsorption Kinetics

Contact time is one of the key parameters in the design of adsorption systems. The effect of contact time on the removal efficiency of heavy metals was investigated over a range of 5–30 minutes (pH = 3, adsorbent dosage: 0.5 g/L). The results are presented in Figure 4.

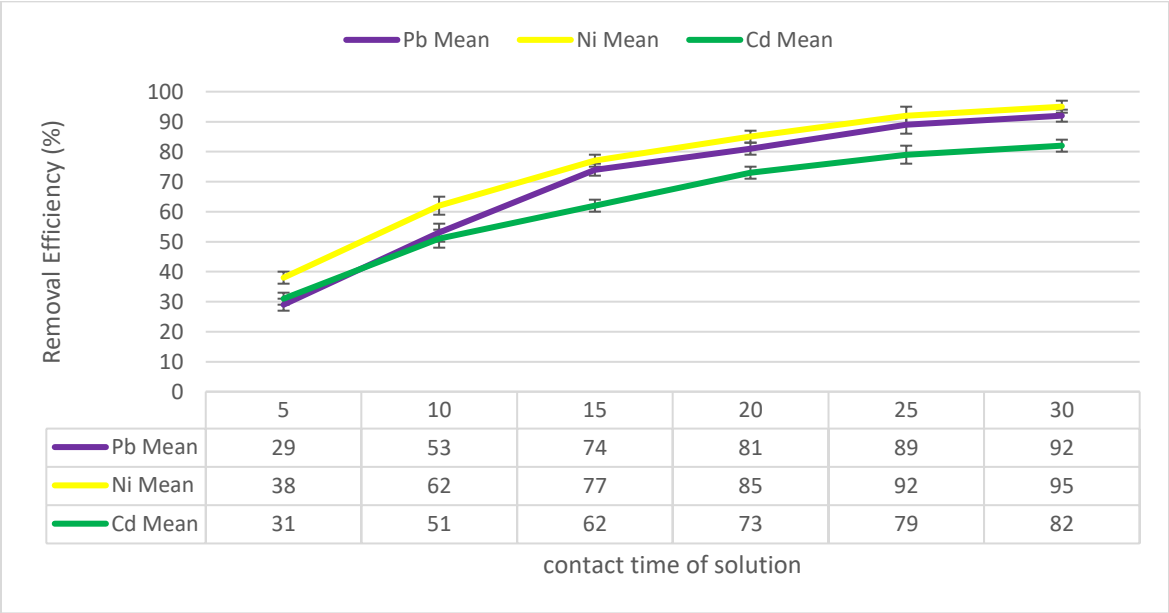

Figure 5. Effect of contact time on the removal efficiency of Pb (II), Ni (II), and Cd (II) by Fe_3O_4 magnetic nanoparticles (pH=3, adsorbent dose: 0.5 g/L, initial concentrations: Pb=17 mg/L, Ni=36 mg/L, Cd=8 mg/L, temperature: 25±2°C, n=5).

The removal efficiency of all three metals increased rapidly during the initial minutes of the adsorption process. Within the first 5 minutes, the removal efficiencies of lead, nickel, and cadmium reached 29%, 38%, and 31%, respectively. This rapid increase can be attributed to the availability of a large number of vacant adsorption sites on the nanoparticle surface and the high concentration gradient between the solution and the adsorbent surface [8,13].After 30 minutes, the adsorption process reached equilibrium, and the removal efficiencies of lead, nickel, and cadmium were reported as 92%, 95%, and 82%, respectively.To investigate the rate-controlling mechanism of adsorption, the experimental data were fitted to two commonly used kinetic models (Eqs. 3 and 4):

❖ Pseudo-First-Order Model

$$\log(q_e - q_t) = log q_e - \frac{k_1}{2.303} t \quad (3)$$

❖ Pseudo-Second-Order Model

$$\frac{t}{q_t} = \frac{1}{k_2 q_e^2} + \frac{t}{q_e} \quad (4)$$

where q_e is the adsorption capacity at equilibrium, q_t is the adsorption capacity at time t, k_1 is the pseudo-first-order rate constant, and k_2 is the pseudo-second-order rate constant. The calculated kinetic parameters and correlation coefficients (R^2) are presented in Table 3.

Table 3. Kinetic parameters for the adsorption of heavy metals onto Fe_3O_4 nanoparticles.

Metal	q_e,exp (mg/g)	Pseudo-first-order			Pseudo-second-order		
		q_e,cal (mg/g)	k_1 (min^{-1})	R^2	q_e,cal (mg/g)	k_2 (g/mg.min)	R^2
Pb(II)	3.13	2.21	0.082	0.921	3.18	0.054	0.997
Ni(II)	6.84	4.92	0.091	0.934	6.89	0.029	0.998
Cd(II)	1.26	0.89	0.075	0.908	1.28	0.118	0.996

As observed, the pseudo-second-order model provided a better description of the experimental data, with higher correlation coefficients (R^2 > 0.99) and closer agreement between the calculated and experimental q_e values. This result indicates that the adsorption process is predominantly controlled by a chemisorption mechanism involving electron sharing or exchange between the metal ions and the functional groups present on the nanoparticle surface [13, 24].

5. Adsorption Isotherms

Adsorption isotherms provide important information regarding the maximum adsorption capacity, the type of interaction between the adsorbent and adsorbate, and the surface homogeneity of the adsorbent [8,15]. The equilibrium adsorption data were fitted to two commonly used isotherm models (Eqs. 5 and 6): Langmuir and Freundlich.

❖ Langmuir Model

$$\frac{C_e}{q_e} = \frac{1}{q_m K_L} + \frac{C_e}{q_m} \quad (5)$$

❖ Freundlich Model

$$logq_e = logK_F + \frac{1}{n} logC_e \quad (6)$$

$R_L$where C_e is the equilibrium concentration of the metal in solution, q_e is the adsorption capacity at equilibrium, q_m is the maximum monolayer adsorption capacity, K_l is the Langmuir constant, Kf is the Freundlich constant, and n is the adsorption intensity constant. The correlation coefficients indicated that the Langmuir model (R^2 > 0.98) described the experimental data better than the Freundlich model (R^2 = 0.92–0.95). This finding suggests that the adsorption of heavy metals onto iron oxide nanoparticles mainly occurs as monolayer adsorption on homogeneous surface sites [19,21]. The maximum adsorption capacities for lead, nickel, and cadmium were calculated as 3.42, 7.28, and 1.41 mg/g, respectively. The n values obtained from the Freundlich model ranged from 2 to 4 for all three metals, indicating favorable adsorption conditions (n > 1 represents favorable adsorption) [22]. The dimensionless separation factor (R_L)in the Langmuir model was calculated using the following equation:

$$R_L = \frac{1}{1+K_L C_0} \quad (7)$$

The calculated R_L values for all three metals ranged between 0 and 1 (0.11–0.47), indicating favorable and feasible adsorption behavior [13].

Table 4. Isotherm parameters for the adsorption of heavy metals onto Fe_3O_4 nanoparticles.

Metal	Langmuir				Freundlich		
	q_m (mg/g)	K_L (L/mg)	R_L	R^2	K_F (mg/g)	n	$\boldsymbol{R^2}$
Pb(II)	3.42	0.185	0.24	0.989	1.12	2.81	0.941
Ni(II)	7.28	0.221	0.11	0.993	2.34	3.15	0.928
Cd(II)	1.41	0.142	0.47	0.981	0.48	2.53	0.935

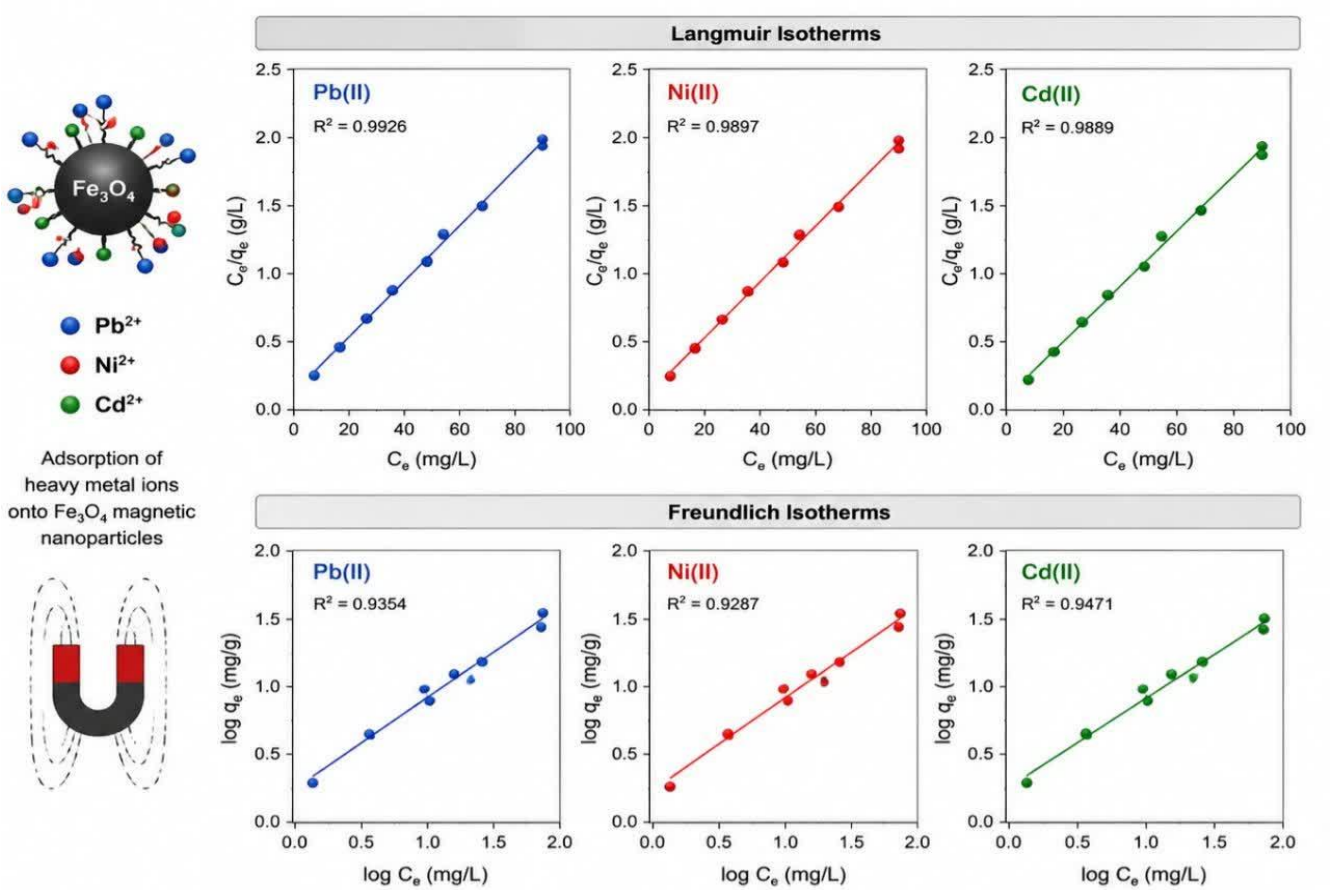

Figure 6. Langmuir and Freundlich isotherm plots for the adsorption of Pb(II), Ni(II), and Cd(II) onto Fe_3O_4 magnetic nanoparticles (pH=3, adsorbent dose: 0.5 g/L, contact time: 30 min, temperature: 25±2°C, n=5).

6. Comparison of the Removal Efficiency of Different Metals

Under optimum conditions (pH = 3, adsorbent dosage: 0.5 g/L, contact time: 30 min), the removal efficiency and adsorption capacity of the three investigated heavy metals are compared in Table 5. Also table 6 summarizes the performance of the unmodified Fe_3O_4 nanoparticles used in the present study in comparison with previously reported adsorbents and separation systems. The comparison shows that the present adsorbent provides high removal efficiencies for Pb(II), Ni(II), and Cd(II), together with a relatively short equilibrium time and low adsorbent dosage. However, differences in pollutants, operating conditions, and experimental matrices should be considered when interpreting these results.

Table 5. Comparison of removal efficiency and adsorption capacity for different heavy metals under optimum conditions

Adsorption Capacity (mg/g)	Removal Efficiency (%)	Final Conc. (mg/L)	Initial Conc. (mg/L)	Metal
Pb(II)	17	0.51	97	3.3
Ni(II)	36	0.72	98	7.06
Cd(II)	8	0.72	91	1.46

Table 6. Comparison of the present Fe_3O_4 nanoparticles with previously reported adsorbents/separation systems.

Adsorbent	**Pollutant**	**Removal efficiency**	**Adsorption capacity**	**Equilibrium / contact time**	**Dosage**	**Operating conditions**	**Reference**
Unmodified Fe_3O_4 nanoparticles (present work)	Pb(II), Ni(II), Cd(II)	97%, 98%, 91%	3.42, 7.28, 1.41 mg/g	25–30 min	0.5 g/L	pH 3; 25±2 °C	Present study
Ionic-liquid-modified nano-clay	Cd(II)	-	87.46–94.6 mg/g	Up to 80 min	4 g/L	Aqueous phase; modified bentonite/montmorillonite	[16]
Ionic-liquid-modified nano-clay	Pb(II), Hg(II)	-	Maximum capacity depends on clay/ionic liquid	80 min	4 g/L	pH investigated 2–10; modified bentonite/montmorillonite	[28]
Zinc powder (cementation)	Ni(II), Cd(II)	>99% for both at optimum	Not reported as adsorption capacity	56.3 min	2 g/L	84.77 °C; pH 4.79; 465.96rpm	[29]
Magnetized tomato-residue nanoadsorbent	Ni(II)	High removal; exact percentage not stated in	83 mg/g	25 min	1.8 g/L	pH 5; 60 °C; initial Ni 60mg/L	[30]
Ag-assisted ionic-liquid microextraction	Ponceau 4R	92–93%	Not an adsorption-capacity metric; preconcentration factor ≈120	Optimized extraction time	Not directly comparable	Response-surface optimization; real pharmaceutical/environmental samples	[31]

Conclusion

Magnetic Fe_3O_4 nanoparticles (18 nm) were evaluated for the simultaneous removal of Pb(II), Ni(II), and Cd(II). Under the investigated conditions, pH = 3 and an adsorbent dosage of 0.5 g/L provided the highest removal efficiencies, reaching 97%, 98%, and 91% for Pb(II), Ni(II), and Cd(II), respectively. Adsorption reached equilibrium within 25–30 min, the kinetic data were best described by the pseudo-second-order model, and the Langmuir model provided the best fit to the equilibrium data, with maximum adsorption capacities of 3.42, 7.28, and 1.41 mg/g for Pb(II), Ni(II), and Cd(II), respectively. The unmodified nanoparticles also allowed rapid magnetic separation. The present study was limited to the three investigated metal ions; evaluation of additional ions, repeated regeneration cycles, and long-term performance in continuous-flow and more complex wastewater matrices is recommended for future work.

References

[1] J. Briffa, E. Sinagra, R. Blundell, Heavy metal pollution in the environment and their toxicological effects on humans. Heliyon., 6 (2020) 1-26.

[2] K. Rehman, F. Fatima, I. Waheed, M.S.H. Akash, Prevalence of exposure of heavy metals and their impact on health consequences. J. Cell. Biochem., 119 (2018) 157-184.

[3] H. Ali, E. Khan, I. Ilahi, Environmental chemistry and ecotoxicology of hazardous heavy metals: Environmental persistence, toxicity, and bioaccumulation. J. Chem., 2019 (2019) 101-118.

[4] C.F. Carolin, P.S. Kumar, A. Saravanan, G.J. Joshiba, M. Naushad, Efficient techniques for the removal of toxic heavy metals from aquatic environment: A review. J. Environ. Chem. Eng., 5 (2017)2782-2799.

[5] F. Fu, Q. Wang, Removal of heavy metal ions from wastewaters: A review. J. Environ. Manage., 92 (2011) 407-418.

[6] A. Azimi, A. Azari, M. Rezakazemi, M. Ansarpour, Removal of heavy metals from industrial wastewaters: A review. ChemBioEng Rev., 4 (2017) 361-377.

[7] R.A.K. Rao, M. Kashifuddin, Adsorption studies of Cd(II) on ball clay: Comparison with other natural clays. Arab. J. Chem., 9 (2016) 1233-1241.

[8] A.E. Burakov, E.V. Galunin, I.V. Burakova, A.E. Kucherova, S. Agarwal, A.G. Tkachev, V.K. Gupta, Adsorption of heavy metals on conventional and nanostructured materials for wastewater treatment purposes: A review. Ecotoxicol. Environ. Saf., 148 (2018) 702-712.

[9] M. Hua, S. Zhang, B. Pan, W. Zhang, L. Lv, Q. Zhang, Heavy metal removal from water/wastewater by nanosized metal oxides: A review. J. Hazard. Mater., 212 (2012) 317-331.

[10] I. Gehrke, A. Geiser, A. Somborn-Schulz, Innovations in nanotechnology for water treatment. Nanotechnol. Sci. Appl., 8 (2015) 1–17.

[11] X. Qu, P.J.J. Alvarez, Q. Li, Applications of nanotechnology in water and wastewater treatment. Water Res., 47 (2013) 3931-3946.

[12] R.D. Ambashta, M. Sillanpää, Water purification using magnetic assistance: A review. J. Hazard. Mater., 180 (2010) 38-49.

[13] P. Xu, G.M. Zeng, D.L. Huang, C.L. Feng, S. Hu, M.H. Zhao, C. Lai, Z. Wei, C. Huang, G.X. Xie, Z.F. Liu, Use of iron oxide nanomaterials in wastewater treatment: A review. Sci. Total Environ., 424 (2012) 1–10.

[14] A.S.K. Kumar, S.-J. Jiang, Chitosan-functionalized graphene oxide: A novel adsorbent an efficient adsorption of arsenic from aqueous solution. J. Environ. Chem. Eng.,

4 (2016) 1698-1713.

[15] L. Li, L. Fan, M. Sun, H. Qiu, X. Li, H. Duan, C. Luo, Adsorbent for chromium removal based on graphene oxide functionalized with magnetic cyclodextrin–chitosan. Colloids Surf. B Biointerfaces, 107 (2013) 76-83.

[16] A. Naderi, M.A. Delavar, Y. Ghorbani, B. Kaboudin, M. Hosseini, Modification of nano-clays with ionic liquids for the removal of Cd (II) ion from aqueous phase. Appl. Clay Sci., 158 (2018) 236-245.

[17] X. Zhao, L. Lv, B. Pan, W. Zhang, S. Zhang, Q. Zhang, Polymer-supported nanocomposites for environmental application: A review. Chem. Eng. J., 170 (2011) 381-394.

[18] S. Zhang, H. Niu, Y. Cai, X. Zhao, Y. Shi, Arsenite and arsenate adsorption on coprecipitated bimetal oxide magnetic nanomaterials: $MnFe_2O_4$ and $CoFe_2O_4$. Chem. Eng. J., 158 (2010) 599-607.

[19] A.O. Dada, A.P. Olalekan, A.M. Olatunya, O. Dada, Langmuir, Freundlich, Temkin and Dubinin–Radushkevich isotherms studies of equilibrium sorption of Zn^{2+} unto phosphoric acid modified rice husk. IOSR J. Appl. Chem., 3 (2012) 38-45.

[20] M. Ghaedi, S. Hajati, F. Karimi, B. Barazesh, G. Ghezelbash, Equilibrium, kinetic and isotherm of some metal ion removal using tree leaf ash as a low cost adsorbent. Korean J. Chem. Eng., 19 (2013) 1047-1053.

[21] L. Largitte, R. Pasquier, A review of the kinetics adsorption models and their application to the adsorption of lead by an activated carbon. Chem. Eng. Res. Des., 109 (2016) 495-504.

[22] T. Madrakian, A. Afkhami, M. Ahmadi, H. Bagheri, Removal of some cationic dyes from aqueous solutions using magnetic-modified multi-walled carbon nanotubes. J. Hazard. Mater., 196 (2011) 109-114.

[23] N.N. Nassar, Rapid removal and recovery of Pb (II) from wastewater by magnetic nano adsorbents. J. Hazard. Mater., 184 (2010) 538-546.

[24] A. Afkhami, M. Saber-Tehrani, H. Bagheri, Simultaneous removal of heavy-metal ions in wastewater samples using nano-alumina modified with 2,4-dinitrophenylhydrazine. J. Hazard. Mater., 181 (2010) 836-844.

[25] R.A. Crane, T.B. Scott, Nanoscale zero-valent iron: Future prospects for an emerging water treatment technology. J. Hazard. Mater., 211 (2012) 112-125.

[26] S. Iravani, Green synthesis of metal nanoparticles using plants. Green Chem., 13 (2011) 2638-2650.

[27] D.H.K. Reddy, S.-M. Lee, Magnetic biochar composite: Facile synthesis, characterization, and application for heavy metal removal. Colloids Surf. A Physicochem. Eng. Asp., 454 (2014) 96-103.

[28] A. Naderi, M.A. Delavar, Y. Ghorbani, M. Hosseini, Development of surface reaction of nano-colloid minerals using novel ionic liquids and assessing their removal ability for Pb (II) and Hg (II). Arab. J. Geosci., 13 (2020) 381-402.

[29] P. Abbasi, K. Shayesteh, V. Vahid Fard, M. Hosseini, Optimization of the nickel removal process from zinc sulfate solution using central composite design of experiments. Iran. J. Anal. Chem., 8 (2021) 17–28.

[30] P. Rani, R. Johar, P.S. Jassal, Adsorption of nickel (II) ions from wastewater using glutaraldehyde cross-linked magnetic chitosan beads: isotherm, kinetics and thermodynamics. Water Sci. Technol., 82 (2020) 2193-2202.

[31] M. Hosseini, S. Shakibafar, T. Saki, Engineering and process optimization of a novel Ag-assisted separation system using a naphthalene-based functional ionic liquid for

the removal of organic dyes. Ind. Eng. Chem. Res., 65 (2026) 8948-8961.

[32] M. Fu, Q. Zhang, B. Li, et al., Removal of heavy metal ions from wastewaters: A review. J. Environ. Manage., 92 (2011) 407-418.

[33] M.A. Barakat, New trends in removing heavy metals from industrial wastewater. Arab. J. Chem., 4 (2011) 361-377.

[34] P.B. Tchounwou, C.G. Yedjou, A.K. Patlolla, D.J. Sutton, Heavy metal toxicity and the environment. Experientia Suppl., 101 (2012) 133-164.

[35] N.A.A. Qasem, R.H. Mohammed, D.U. Lawal, Removal of heavy metal ions from wastewater: A comprehensive and critical review. npj Clean Water, 4 (2021) 36-50.

https://ijac.journals.pnu.ac.ir/

نشریه ایرانی شیمی تجزیه

سال سیزدهم، شماره یکم، بهار ۱۴۰۵، صفحات ۹۳–۱۰۸

DOI: 10.30473/ijac.2026.78706.1354

دسترسی آزاد

دانشگاه پیام نور

Iranian Journal of Analytical Chemistry

مقاله پژوهشی

ارزیابی کارایی نانوذرات مغناطیسی اکسید اهن در حذف فلزات سنگین از فاضلاب صنعتی

حمید یزدانی ✉

دانشیار، گروه مهندسی شیمی، دانشگاه پیام نور، تهران، ایران.

✉ نویسنده مسئول:
حمید یزدانی
رایانامه: h.yazdani@pnu.ac.ir

تاریخ دریافت: ۱۴۰۵/۰۵/۳۰
تاریخ پذیرش: ۱۴۰۵/۰۷/۱۹

چکیده

فلزات سنگینی مانند سرب، نیکل و کادمیوم موجود در پساب‌های صنعتی، خطرات جدی برای محیط زیست و سلامت عمومی ایجاد می‌کنند. در این مطالعه، نانوذرات اکسید آهن مغناطیسی با اندازه کریستالیت ۱۸ نانومتر به روش هم‌رسوبی سنتز شده و کارایی آن‌ها برای حذف همزمان یون‌های Pb(II)، Ni(II) و Cd(II) از محلول‌های آبی ارزیابی شد. مشخصه‌یابی نانوذرات با استفاده از روش‌های پراش پرتو ایکس (XRD)، میکروسکوپ نوری و اندازه‌گیری‌های مغناطیسی انجام گرفت. آزمایش‌های جذب ناپیوسته (Batch) در دمای ۲۵ درجه سانتی‌گراد برای بررسی تأثیرات pH (۳ تا ۹)، مقدار جاذب (۰٫۳ تا ۱٫۰ گرم بر لیتر) و زمان تماس (۵ تا ۳۰ دقیقه) اجرا شد. نوآوری اصلی این پژوهش، دستیابی به بازده حذف بالا در شرایط اسیدی (pH = 3) بدون نیاز به هیچ‌گونه اصلاح سطحی است: ۹۷٪ برای Pb(II)، ۹۸٪ برای Ni(II) و ۹۱٪ برای Cd(II)؛ که این امر نشان‌دهنده پتانسیل بالای این نانوذرات برای تصفیه پساب‌های صنعتی اسیدی بدون نیاز به تنظیم pH می‌باشد. افزایش pH به ۹، بازده حذف را به ۴۵٪ برای Pb(II)، ۵۸٪ برای Ni(II) و ۴۱٪ برای Cd(II) کاهش داد. مقدار بهینه جاذب ۰٫۵ گرم بر لیتر تعیین شد؛ مقادیر بالاتر به دلیل تجمع (کلوخه شدن) ذرات، موجب کاهش بازده گردید. تعادل جذب در مدت ۲۵ تا ۳۰ دقیقه حاصل شد. داده‌های سینتیکی انطباق بسیار خوبی با مدل شبه‌مرتبه دوم نشان دادند، در حالی که داده‌های تعادلی به خوبی با ایزوترم لانگمویر توصیف شدند که بیانگر وقوع فرآیند شیمی‌جذب تک‌لایه بر روی سایت‌های جذب همگن است. حداکثر ظرفیت‌های جذب برای یون‌های Pb(II)، Ni(II) و Cd(II) به ترتیب برابر با ۳٫۴۲، ۷٫۲۸ و ۱٫۴۱ میلی‌گرم بر گرم تعیین گردید. قابلیت جداسازی مغناطیسی سریع و امکان استفاده مجدد، این نانوذرات را به جاذبی کارآمد و مقرون‌به‌صرفه برای تصفیه پساب‌های صنعتی تبدیل کرده است.

واژه‌های کلیدی

نانوذرات اکسید آهن؛ حذف فلزات سنگین؛ تصفیه فاضلاب؛ جذب؛ جداسازی مغناطیسی؛ پساب صنعتی.

استناد به این مقاله:

یزدانی، حمید. (۱۴۰۵). ارزیابی کارایی نانوذرات مغناطیسی اکسید اهن در حذف فلزات سنگین از فاضلاب صنعتی. *نشریه ایرانی شیمی تجزیه*، ۱۳(۱) ۹۳–۱۰۸.
(DOI: 10.30473/ijac.2026.78706.1354)

حق انتشار این مستند، متعلق به نویسندگان آن است. ۱۴۰۵ ©. ناشر این مقاله، دانشگاه پیام نور است.

این مقاله تحت گواهی زیر منتشرشده و هر نوع استفاده غیرتجاری از آن مشروط بر استناد صحیح به مقاله و با رعایت شرایط مندرج در آدرس زیر مجاز است.

Creative Commons Attribution-NonCommercial 4.0 International license (https://creativecommons.org/licenses/by-nc/4.0/)